Betacellulin and Amphiregulin Induce Upregulation of Cyclin D1 and DNA Synthesis Activity Through Differential Signaling Pathways in Vascular Smooth Muscle Cells

Hyoung Seek Shin, Hyo Jeong Lee, Makoto Nishida, Mi-Sook Lee, Ritsu Tamura, Shizuya Yamashita, Yuji Matsuzawa, In-Kyu Lee, Gou Young Koh

Abstract—Activation of EGF receptors is closely involved in vascular proliferative diseases. The signaling mechanisms of EGF ligands, including betacellulin (BTC) and amphiregulin (AR), are poorly understood. We examined how BTC and AR induced DNA synthesis activity in primary cultures of human thoracic aortic smooth muscle cells (HTASMCs). BTC induced phosphorylation of all four EGF receptors present on HTASMCs: ErbB1, ErbB2, ErbB3, and ErbB4. BTC rapidly induced the phosphorylation of Akt, GSK3α/β, and two FoxO factors, FKHR and AFX, in a dose- and time-dependent manner. BTC increased nuclear β-catenin accumulation. BTC increased cyclin D1 mRNA, cyclin D1 protein, and DNA synthesis activity. Pretreatment with the phosphatidylinositol 3′-kinase (PI 3′-kinase) inhibitor wortmannin suppressed BTC-induced cyclin D1 mRNA and protein and DNA synthesis activity. In contrast, AR, a specific ErbB1 ligand, induced sustained ERK1/2 and Elk1 phosphorylation, increased cyclin D1 mRNA and protein, and increased DNA synthesis activity. AR did not produce any changes in Akt phosphorylation. Pretreatment with PD98059 suppressed AR-induced cyclin D1 mRNA and protein. Thus, the PI 3′-kinase/Akt/GSK/FoxO/β-catenin pathway could be the major signaling cascade for BTC-induced upregulation of cyclin D1 protein, whereas a sustained ERK/Elk1 activation could be the major signaling cascade for AR-induced upregulation of cyclin D1 protein in HTASMCs. Moreover, immunohistochemical staining revealed that that BTC, ErbB1, and ErbB4 are upregulated in the plaques of human atherosclerotic coronary arteries. Taken together, BTC and AR could be potent growth factors in proliferative vascular diseases. **(*Circ Res*. 2003;93:302-310.)**

Key Words: betacellulin ■ amphiregulin ■ epidermal growth factor receptors ■ phosphatidylinositol 3′-kinase ■ extracellular signal-regulated kinase 1 and 2

Betacellulin (BTC) and amphiregulin (AR) are members of the EGF family. BTC was originally identified as a growth-promoting factor in the conditioned medium of a mouse pancreatic β-cell carcinoma (insulinoma) cell line,[1] and it has since been identified in humans.[2] AR was originally identified from conditioned medium of a phorbol 12-myristate 13-acetate–treated human breast carcinoma cell line.[3] BTC has been shown to be a potent mitogen for fibroblasts, vascular smooth muscle cells (VSMCs), and retinal pigment epithelial cells, whereas AR is a cell type–dependent bifunctional modulator of cell growth.[1,3] BTC and AR are synthesized in a wide range of adult tissues and in many cultured cells, including smooth muscle cells and epithelial cells.[1–4]

Four EGF receptors are currently known: ErbB1 (EGFR), ErbB2 (HER2/neu), ErbB3 (HER3), and ErbB4 (HER4).[5–7] The receptors exist as inactive monomers that dimerize after ligand activation, either as homo- or heterodimers. After ligand binding, the tyrosine kinase intracellular domain of the receptor is activated, with autophosphorylation of the intracellular domain; the phosphorylated receptor then initiates a cascade of intracellular events.[5–7] BTC is known to bind and stimulate homodimers of ErbB1 and ErbB4, and heterodimers of ErbB1/ErbB2, ErbB1/ErbB3, ErbB1/ErbB4, ErbB2/ErbB3, and, ErbB2/ErbB4.[5–8] AR is known to preferentially bind and stimulate homodimers of ErbB1.[6] Thus, BTC and AR produce physiological and pathological effects through ErbB receptors, although their binding and affinity vary among different cell types.

Recently, we showed that BTC induced angiogenesis in primary cultured endothelial cells through the activation of ErbB2, ErbB3, and ErbB4 receptors acting on two pathways: the intracellular phosphatidylinositol 3′-kinase (PI 3′-kinase)/Akt pathway and the extracellular signal-regulated kinase 1 and 2 (ERK1/2) pathway.[9] We also observed that BTC-

Original received March 6, 2003; revision received July 7, 2003; accepted July 8, 2003.

From the National Creative Research Initiatives Center for Endothelial Cells and Division of Molecular and Life Sciences (H.S.S., MSL., G.Y.K.), Pohang University of Science and Technology, Pohang, Korea; Department of Internal Medicine (H.J.L, I-K.L.), Keimyung University School of Medicine, Taegu, Korea; and the Department of Internal Medicine and Molecular Science (M.N., R.T., Y.M., S.Y.), Graduate School of Medicine, Osaka University, Yamada-Oka, Suita, Osaka, Japan.

Correspondence to Gou Young Koh, MD, PhD, National Creative Research Initiatives Center for Endothelial Cells, Division of Molecular and Life Sciences, Pohang University of Science and Technology, San 31, Hyoja-Dong, Pohang, 790-784, Republic of Korea. E-mail gykoh@postech.ac.kr

Circulation Research **is available at http://www.circresaha.org** **DOI: 10.1161/01.RES.0000086803.64109.9E**

immunopositive VSMCs are more abundant in the intimal region of atherosclerotic lesions than in the normal portions of human thoracic aortas.[10] Notably, strong BTC-immunoreactivity in the migrating VSMCs and macrophages were observed around the core lesion of atherosclerotic plaques, suggesting that BTC may be closely involved in vascular proliferative diseases. Moreover, recent studies indicate that activation of PI 3′-kinase is the key signaling pathway for induction of cyclin D1 and cell cycle in VSMCs in animal models of vascular proliferation.[11,12]

Therefore, in this study, we examined how BTC and AR induced DNA synthesis activity in primary cultures of human thoracic aortic smooth muscle cells (HTASMCs). In addition, we reevaluated the localization of BTC and its receptors in atherosclerotic lesions of human coronary artery. Our results indicate that BTC and AR could be potent growth factors for proliferative vascular diseases.

Materials and Methods

Materials and Cell Culture

Recombinant human BTC and AR were purchased from Sigma-Aldrich. Recombinant human EGF was purchased from R&D Systems. PI 3′-kinase inhibitor wortmannin, Akt inhibitor, and mitogen-activated protein/extracellular signal-regulated kinase (MEK) 1/2 inhibitor PD98059 were purchased from Calbiochem. Antibodies for phosphospecific Akt (Ser473), GSK3α/β (Ser21/Ser9), FKHR (Ser256)/AFX, Elk1 (Ser383), and ERK1/2 (Thr202/Tyr204) were purchased from Cell Signaling Technology. Antibodies for ErbB1, ErbB2, ErbB3, ErbB4, and cyclin D1 were purchased from Santa Cruz Biotechnology. Antibodies for phospho-ErbB1, phospho-ErbB2, and phospho-tyrosine were purchased from Upstate Biotechnology. Antibody for β-catenin was purchased from BD Transduction Laboratories. HTASMCs were isolated from thoracic aortas of donors during heart transplant by the explant method and were cultured as described previously.[13] Tissue collection was approved by the local Ethics Committee of Keimyung University Hospital. The primary cultured cells used in this study were between passage 3 and 5.

Biochemical Analyses

HTASMCs were incubated in DMEM with 1% fetal bovine serum for 16 hours before addition of the indicated growth factors. The phosphorylation of EGF receptors, Akt, GSK3α/β, FoxO factors, ERK1/2 and Elk1, and the protein levels of β-catenin and cyclin D1 were measured as previously described.[9] All signals were visualized and analyzed by densitometric scanning (LAS-1000, Fuji Film).

Confocal Microscopy

HTASMCs were seeded onto glass coverslips and incubated for 24 hours before addition of BTC. Treated cells were washed with PBS, fixed with methanol/acetone (1:1) for 15 minutes, incubated with anti–β-catenin antibody (BD Transduction Laboratories), then incubated with FITC-conjugated secondary antibody, and counterstained with Hoechst 33425. The slides were mounted and examined by confocal microscopy, and images were captured with an LSM 510 camera (Zeiss).

Ribonuclease Protection Assay (RPA)

RPA for human cyclin D1 and cyclophilin were performed on total RNAs using the Ambion RPA kit.

Assays of DNA Synthesis and Cell Cycle Progression

The DNA synthetic activity of HTASMCs was measured using PicoGreen fluorescent reagent (Molecular Probes) as previously described.[9] Cell cycle progression was measured using propidium iodide staining with a FACSCalibur (BD Bioscience).

Sampling and Immunohistochemistry

Human atherosclerotic coronary arteries were obtained from autopsied cadavers with informed consent of the next of kin. Immunohistochemical detection of BTC and EGF receptors in the lesions was performed as described previously.[10]

Data Analyses

Data are expressed as mean±SD. Statistical significance was tested using 1-way ANOVA followed by the Student-Newman-Keuls test. Statistical significance was set at $P<0.05$.

An expanded Materials and Methods section can be found in the online data supplement available at http://www.circresaha.org.

Results

BTC Induced Activation of All Four ErbB Receptors

Because BTC is known to exert biological effects through ErbB receptors,[8] we examined the distribution of subtypes of EGF receptors in primary cultures of HTASMCs. Our Western blot analyses indicated that HTASMCs express all four ErbB receptors, ErbB1, ErbB2, ErbB3, and ErbB4, and that EGF phosphorylated all four receptors (data not shown). Furthermore, BTC phosphorylated all four receptors: ErbB1, ErbB2, ErbB3, and ErbB4 (see online Figure 1 in the online data supplement at http://www.circresaha.org).

BTC Induces Phosphorylation of Akt, GSK3α/β, FKHR, AFX, ERK1/2, and Elk1 and Induces Accumulation of Nuclear β-Catenin

Because growth factor receptors are known to mediate the activation of intracellular PI 3′-kinase/Akt and MEK/ERK cascades for upregulation of cyclin D1 and proliferation,[14] we first examined the effect of BTC on phosphorylation of Akt (Ser473) and ERK1/2 in primary cultured HTASMCs. BTC (10 ng/mL) increased the phosphorylation of Akt and its downstream kinase, GSK3α/β (Ser21/Ser9), as early as 1 minute and produced a maximal effect at 1 minute (Figures 1A and 1B). The phosphorylation level declined but remained higher than control at 30 minutes. The maximum mean increases in Akt and GSK3β phosphorylation were 12.5-fold and 14.6-fold, respectively. BTC (0.03 to 10 ng/mL) increased the phosphorylation of both Akt and GSK3α/β in a dose-dependent manner (Figures 1C and 1D). In addition, pretreatment with PI 3′-kinase inhibitor, wortmannin (30 nmol/L), completely abolished the BTC-induced Akt and GSK3α/β phosphorylation (data not shown). Pretreatment with Akt inhibitor suppressed the BTC-induced GSK3α/β phosphorylation in a dose-dependent manner (Figure 1E). Both BTC (10 ng/mL at 1 minute) and EGF (10 ng/mL at 5 minutes) produced a similar level of Akt and GSK3α/β phosphorylation (Figure 1). Inactivation of GSK3α/β through dephosphorylation at two sites (Ser21/Ser9) is known to cause β-catenin to accumulate in the cytoplasm and then translocate into the nucleus.[15] Accordingly, BTC (10 ng/mL) increased β-catenin protein level as early as 1 minute and produced a continued increase until 60 minutes (Figure 2A). Immunofluorescent staining revealed that more than 60% of BTC-treated cells have a marked increase of β-catenin in the nuclei (Figure 2B). Pretreatment with GSK inhibitor, LiCl

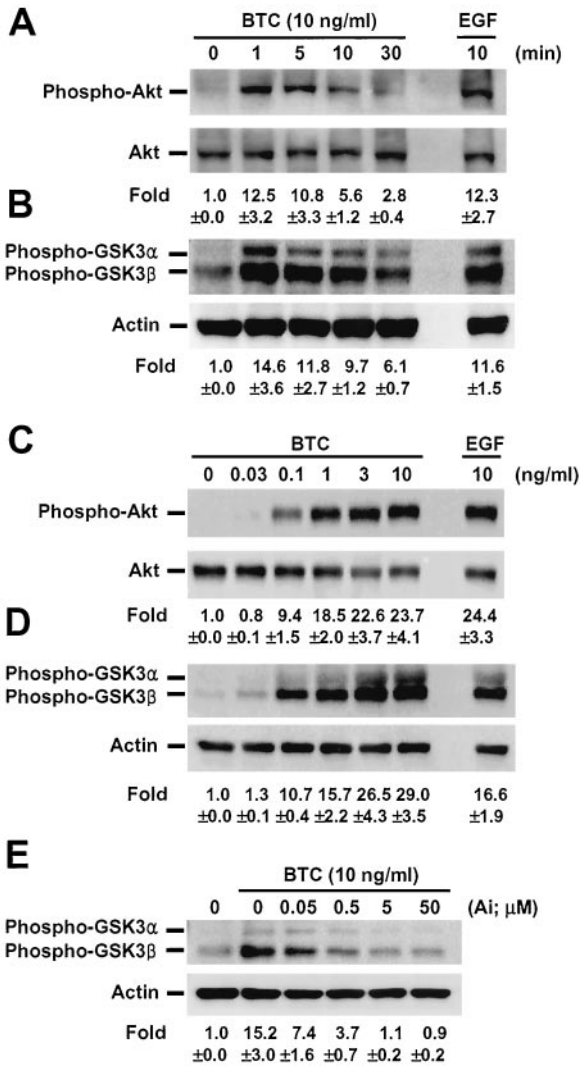

Figure 1. BTC induces phosphorylation of Akt and GSK3α/β. HTASMCs were incubated for 16 hours in medium with 1% serum-containing DMEM, then incubated with BTC (10 ng/mL) or EGF (10 ng/mL) for the indicated times (A and B), or for 1 minute at the indicated concentrations (C and D). Cells were pretreated with the indicated concentrations of Akt inhibitor (Ai) before incubation with BTC (10 ng/mL) for 5 minutes (E). After treatment, cell lysates were harvested. Each lane contains 50 μg of total protein from the cell lysates. Blots were probed with anti–phospho-Akt (Ser473) antibody (A and C) or anti–phospho-GSK3α/β antibody (B and D) (top). Membrane was stripped and reprobed with anti-Akt antibody or anti-actin antibody (bottom) to verify equal loading of protein in each lane. Fold indicates densitometric analyses presented as the relative ratio of phospho-Akt to Akt or phospho-GSK3α/β to actin. Relative ratio measured at time 0, or the ratio relative to control buffer (0), is arbitrarily presented as 1. Numbers represent the mean±SD from 3 experiments.

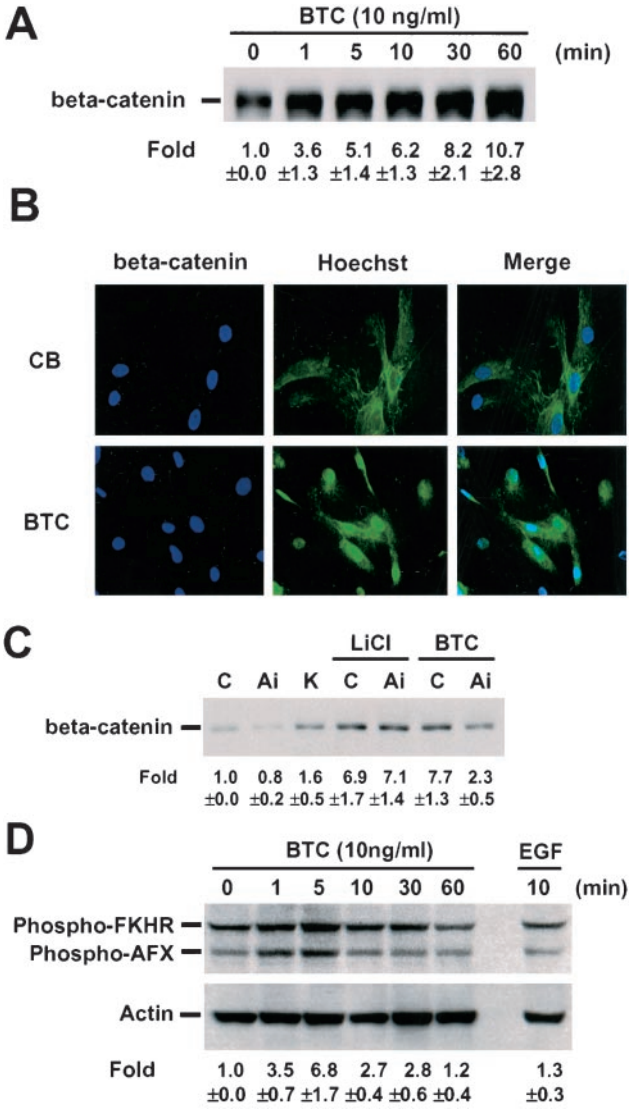

Figure 2. BTC increases β-catenin protein levels. HTASMCs were incubated for 16 hours in medium with 1% serum-containing DMEM, then incubated with BTC (10 ng/mL) for the indicated times. A and D, Cell lysates were harvested and 50 μg of total protein was used for blotting with anti–β-catenin antibody or anti–phospho-FKHR (Ser256)/AFX antibody. B, Representative confocal micrographs of β-catenin. At 30 minutes after treatment, cells were fixed, then stained with anti–β-catenin antibody and FITC-labeled secondary antibody, and counterstained with Hoechst 33425 for nuclear staining. Note that β-catenin is mainly located in the cytoplasm, but there is a dramatic increase of β-catenin in the nucleus 30 minutes after BTC treatment. C, Cells were pretreated with Akt inhibitor (5 μmol/L) for 1 hour before stimulation with LiCl (20 mmol/L) or BTC (10 ng/mL) for 30 minutes. KCl (K, 20 mmol/L) treatment for 30 minutes was used as a control. After treatment, nuclear fractions were prepared and 50 μg of total protein from the fractions was Western-blotted with anti–β-catenin antibody. Fold indicates densitometric analyses presented as the relative ratio to time 0. The ratio measured at time 0 is arbitrarily presented as 1 in β-catenin or phospho-FKHR. Numbers represent the mean±SD from 3 experiments.

(20 mmol/L), increased nuclear β-catenin protein level regardless of Akt inhibition (Figure 2C). In addition, pretreatment with Akt inhibitor markedly suppressed BTC-induced nuclear β-catenin protein level (Figure 2C). These data indicate that the BTC-induced increase in nuclear β-catenin protein level is mainly through the PI 3′-kinase/Akt/GSK3 cascade in VSMCs. Moreover, BTC increased the phosphorylation of Akt downstream transcription factors, FoxO transcriptional factors FKHR and AFX, in a time-dependent manner (Figure 2D). BTC (10 ng/mL) also increased the phosphorylation of ERK1/2 and its downstream transcription factor, Elk1, as early as 1 minute and produced a maximal

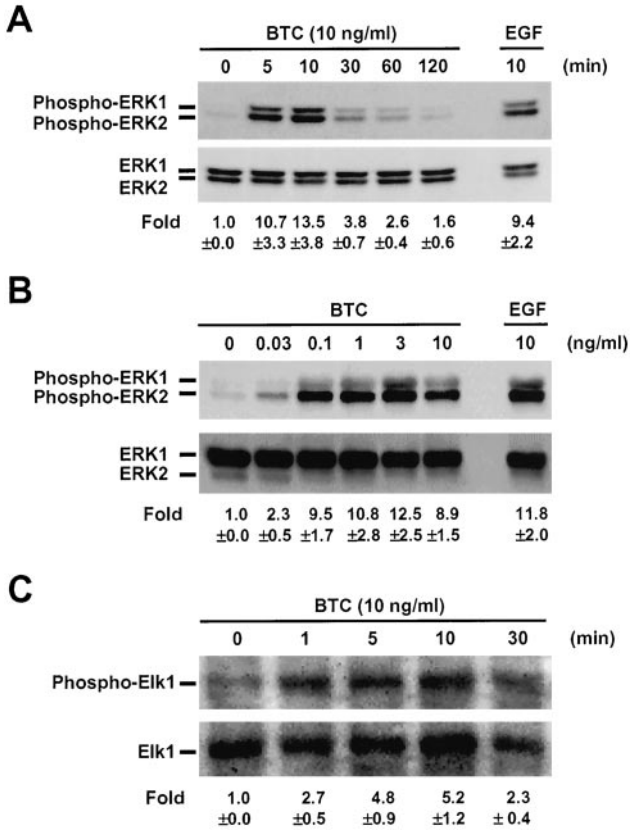

Figure 3. BTC induces phosphorylation of ERK1/2 and Elk1. HTASMCs were incubated for 16 hours in medium with 1% serum-containing DMEM, then incubated with BTC (10 ng/mL) or EGF (10 ng/mL) for the indicated times (A and C), or for 5 minutes at the indicated concentrations (B). After treatment, cell lysates were harvested. Each lane contains 50 μg of total protein from the cell lysates. Blots were probed with anti–phospho-ERK1/2 antibody (A and B) or anti–phospho-Elk1 antibody (C) (top). Membrane was stripped and reprobed with anti-ERK1/2, anti-actin (data not shown), or anti-Elk1 antibody (bottom) to verify equal loading of protein in each lane. Fold indicates densitometric analyses presented as the relative ratio of phospho-ERK2 to actin or phospho-Elk1 to Elk1. Relative ratio measured at time 0, or the ratio relative to control buffer (0), is arbitrarily presented as 1. Numbers represent the mean±SD from 3 experiments.

effect at 10 minutes (Figures 3A and 3C). These effects declined but remained higher than control at 60 minutes. The maximum mean increases in ERK1/2 and Elk1 phosphorylation were 13.5-fold and 5.2-fold, respectively. BTC (0.03 to 10 ng/mL) increased ERK1/2 phosphorylation in a dose-dependent manner (Figure 3B). In addition, pretreatment with MEK inhibitor, PD98059 (50 nmol/L), completely abolished the BTC-induced ERK1/2 and Elk1 phosphorylation (data not shown). Both BTC (10 ng/mL at 10 minutes) and EGF (10 ng/mL at 10 minutes) produced a similar level of ERK1/2 phosphorylation (Figure 3). These data indicate that BTC is a strong activator of both the intracellular Akt/GSK3/FoxO/β-catenin cascade and the ERK/Elk1 cascade in VSMCs.

BTC Upregulates Cyclin D1 Protein Mainly Through the Intracellular PI 3′-Kinase/Akt Pathway

The phosphorylation of Akt, GSKα/β, and FoxO factors, and the accumulation of nuclear β-catenin play a crucial role in the upregulation of cyclin D1 protein level by suppressing cyclin D1 degradation and by increasing cyclin D1 transcription (16 to 19, MCB). Phosphorylation of ERK1/2 plays a crucial role in the upregulation of cyclin D1 protein level by increasing cyclin D1 transcription.[14] Therefore, we next examined how BTC upregulated cyclin D1 protein levels in HTASMCs. BTC (10 ng/mL) increased cyclin D1 mRNA and protein in a time-dependent manner (Figures 4A and 4B). Interestingly, pretreatment with PI 3′-kinase inhibitor wortmannin (30 nmol/L) almost completely suppressed BTC-induced cyclin D1 mRNA and protein, whereas pretreatment with MEK inhibitor PD98059 (50 nmol/L) only weakly suppressed these increases (Figures 4C and 4D). Moreover, pretreatment with Akt inhibitor completely suppressed BTC-induced cyclin D1 protein. Thus, PI 3′-kinase/Akt/GSK/FoxO/β-catenin appears to be the major regulatory pathway for BTC-induced upregulation of cyclin D1 protein in VSMCs.

AR Upregulates Cyclin D1 Protein Mainly Through Sustained Activation of the Intracellular ERK/Elk1 Pathway

Because activation of different ErbB receptors is known to activate different intracellular signaling cascades, we examined the effect of specific ErbB1 ligand, AR, on signaling cascades and cyclin D1 levels in HTASMCs. Preliminary results indicated that 100 ng/mL of AR produced a maximal effect in ErbB1 and ERK1/2 phosphorylation (data not shown). Thus, we chose this concentration of AR for the subsequent experiments. As expected, AR (100 ng/mL) phosphorylated only ErbB1 among four ErbB receptors (Figures 5A through 5C). Notably, AR (100 ng/mL) did not produce any changes in Akt (Ser473) phosphorylation up to 60 minutes (Figure 5D). In contrast, AR (100 ng/mL) increased ERK1/2 and Elk1 phosphorylation as early as 1 minute and produced a maximal effect at 60 minutes (Figures 5E and 5F). These effects declined slightly but remained elevated up to 5 hours (data not shown). The maximum mean increases in ERK1/2 and Elk1 phosphorylation were 12.8-fold and 11.1-fold, respectively. Thus, AR-induced ERK/Elk1 activation was more sustained than BTC-induced ERK/Elk1 activation. AR (100 ng/mL) increased cyclin D1 mRNA in a time-dependent manner, whereas it increased cyclin D1 protein at 6 hours and maintained the same elevated levels of cyclin D1 protein at 12 and 24 hours after treatment (Figures 6A and 6B). In comparison, BTC (10 ng/mL) steadily increased cyclin D1 protein. Accordingly, pretreatment with PD98059 (50 nmol/L) markedly suppressed AR-induced cyclin D1 mRNA and protein, whereas pretreatment with wortmannin (30 nmol/L) slightly suppressed AR-induced cyclin D1 mRNA and protein (Figures 6C and 6D). Thus, AR-induced ErbB1 activation produced a sustained ERK/Elk1 activation, which could be a major regulator for AR-induced upregulation of cyclin D1 protein in VSMCs.

BTC and AR Increased DNA Synthetic Activity and Cell Cycle Progression Through Different Signaling Pathways

Because upregulation of cyclin D1 protein is a major regulatory step in the G1 phase of cell cycle,[20] we examined the

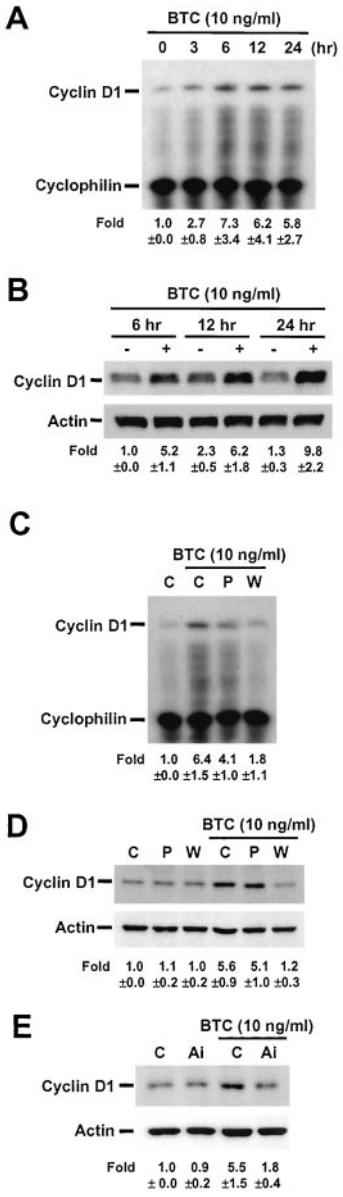

Figure 4. BTC increases cyclin D1 mRNA and protein in a PI 3′-kinase–dependent manner. HTASMCs were incubated for 16 hours in medium with 1% serum-containing DMEM, then incubated with BTC (10 ng/mL) for the indicated times (A and B) or with inhibitors (C, D, and E) for 24 hours. A and C, Total RNAs (10 μg) were subjected to RPA probed with antisense human cyclin D1. Equivalent loading was confirmed by simultaneously probing with an antisense cyclophilin RNA probe. B, D, and E, After treatment, cell lysates were harvested, and 50 μg of total protein from the cell lysates was blotted and probed with anti-cyclin D1 antibody (top). Membrane was stripped and reprobed with anti-actin antibody (bottom) to verify equal loading of protein in each lane. C indicates control buffer; P, PD98059 (50 nmol/L); W, wortmannin (30 nmol/L); Ai, Akt inhibitor (5 μmol/L). Fold indicates densitometric analyses presented as the relative ratio of cyclin D1 mRNA to cyclophilin mRNA or cyclin D1 protein to actin. Relative ratio measured at time 0, or the ratio relative to control, is arbitrarily presented as 1. Numbers represent the mean±SD from 3 experiments.

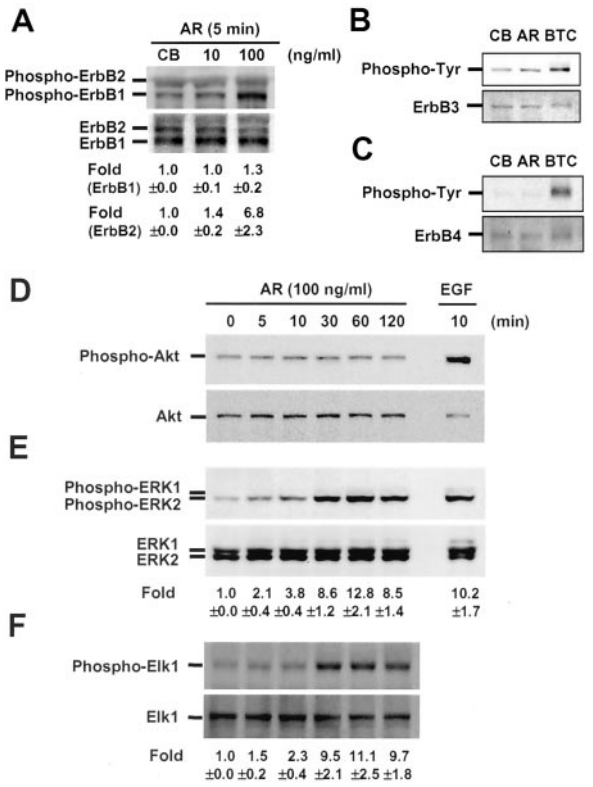

Figure 5. AR induces phosphorylation of ErbB1, ERK1/2, and Elk1, but not ErbB2, ErbB3, ErbB4, and Akt. HTASMCs were incubated for 16 hours in medium with 1% serum-containing DMEM, then incubated with AR for 5 minutes at the indicated concentrations (A), with AR (100 ng/mL) or BTC (10 ng/mL) for 5 minutes (B and C), or with AR (100 ng/mL) or EGF (10 ng/mL) for the indicated times (D, E, and F). A, D, E, and F, After treatment, cell lysates were harvested. Each lane contains 50 μg of total protein from the cell lysates. Blots were probed with anti–phospho-ErbB1/B2, anti–phospho-Akt, anti–phospho-ERK1/2 antibody, or anti–phospho-Elk1 antibody (top). Membrane was stripped and reprobed with anti-ErbB1/B2, anti-Akt, anti-ERK1/2, or anti-Elk1 antibody (bottom) to verify equal loading of protein in each lane. B and C, Cells were harvested in extraction buffer, and 0.5 mg of protein was used for immunoprecipitation with anti-ErbB3 or anti-ErbB4 antibody. Immunoprecipitated samples were blotted with anti-phosphotyrosine antibody (top). Membranes were reprobed with anti-ErbB3 or anti-ErbB4 antibody to verify equal loading of protein in each lane (bottom). Fold indicates densitometric analyses presented as the relative ratio of phospho-ErbB1/2/3/4 to ErbB1/2/3/4, phospho-Akt to Akt, phospho-ERK1/2 to ERK1/2, or phospho-Elk1 to Elk1. Relative ratio measured at time 0, or the ratio relative to control buffer (CB), is arbitrarily presented as 1. Numbers represent the mean±SD from 3 experiments.

effects of BTC and AR on DNA synthesis in HTASMCs. BTC and AR increased DNA synthetic activity approximately 2.9-fold and 1.9-fold, respectively (see online Figure 2A). Moreover, BTC and AR increased cell cycle progression from G1 phase to S and G2/M phase (see online Figure 2). Pretreatment with wortmannin (30 nmol/L) almost completely suppressed BTC-induced DNA synthetic activity and cell cycle progression, whereas pretreatment with PD98059 (50 nmol/L) slightly suppressed BTC-induced DNA synthetic activity and cell cycle progression (see online Figure 2). In contrast, pretreatment with wortmannin (30 nmol/L) slightly suppressed AR-induced DNA synthetic activity and cell cycle progression, whereas PD98059 (50 nmol/L) almost completely suppressed AR-induced DNA synthetic activity and cell cycle progression (see online Figure 2). Thus, BTC-

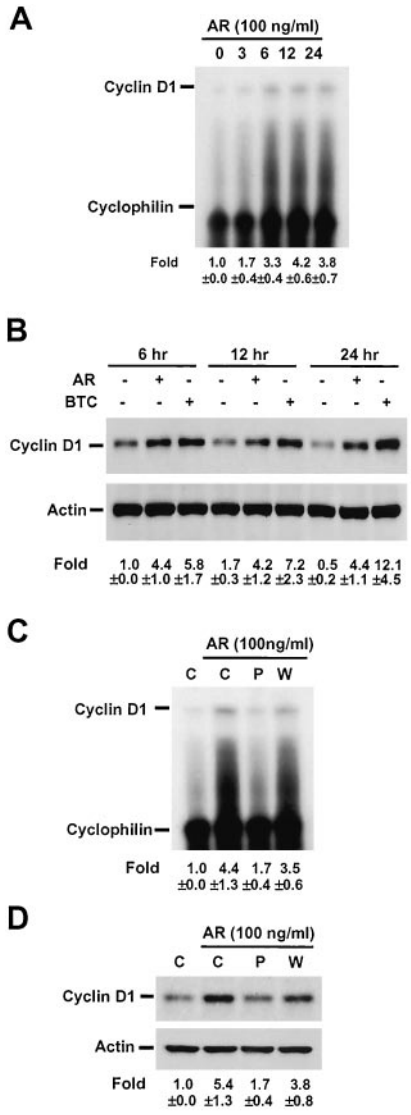

Figure 6. BTC increases cyclin D1 mRNA and protein in a PI 3′-kinase–dependent manner. HTASMCs were incubated for 16 hours in medium with 1% serum-containing DMEM, then incubated with AR (100 ng/mL) or BTC (10 ng/mL) for the indicated times (A and B), or with inhibitors (C and D). A and C, Total RNAs (10 μg) were subjected to RPA probed with antisense human cyclin D1. Equivalent loading was confirmed by simultaneously probing with an antisense cyclophilin RNA probe. B and D, After treatment, cell lysates were harvested and 50 μg of total protein from the lysates was blotted and probed with anti-cyclin D1 antibody (top). Membrane was stripped and reprobed with anti-actin antibody (bottom) to verify equal loading of protein in each lane. C indicates control buffer; P, PD98059 (50 nmol/L); W, wortmannin (30 nmol/L). Fold indicates densitometric analyses presented as the relative ratio of cyclin D1 mRNA to cyclophilin mRNA or cyclin D1 protein to actin. Relative ratio measured at time 0, or the ratio relative to control, is arbitrarily presented as 1. Numbers represent the mean±SD from 3 experiments.

induced DNA synthetic activity and cell cycle progression is mainly dependent on PI 3′-kinase/Akt dependent upregulation of cyclin D1, whereas AR-induced DNA synthetic activity and cell cycle progression is mainly dependent on ERK dependent upregulation of cyclin D1.

BTC and ErbB Are Found in Atherosclerotic Plaques

Given that BTC is a potent factor for DNA synthesis and cell cycle progression, and the antibodies for ErbB1, ErbB2, and ErbB4 work well on paraffin-embedded human tissues, we used immunohistochemistry to evaluate the expression of BTC, ErbB1, ErbB2, and ErbB4 in human atherosclerotic coronary arteries. Consistent with our previous report,[10] in the nonatherosclerotic portion of coronary artery, the intimal VSMCs form diffuse intimal thickening lesions. BTC immunostaining was detected weakly in the medial VSMCs and relatively intensely in the intimal VSMCs near the internal elastic lamina (data not shown). In the atherosclerotic portion of coronary artery, macrophages, macrophage-derived foam cells, lymphocytes, and VSMCs make up eccentric intimal thickening lesions, termed plaques. Strong BTC immunoreactivity was detected in macrophages and VSMCs (Figures 7A, 7B, and 7D). VSMCs, in particular, had BTC immunoreactivity near the inner elastic lamina of the plaque (Figures 7E and 7F). In these lesions, many ErbB1- (Figure 7I) or ErbB4- (Figure 7J) positive cells were observed, whereas ErbB2 immunoreactivities were hardly detected (data not shown). Macrophage-derived foam cells had no immunostaining of ErbB1 and ErbB4. VSMCs around a small vessel were positive for ErbB1 immunostaining (Figures 7H and 7I).

Discussion

BTC is a ligand of multiple EGF receptors and is known to bind to homodimers of ErbB1 and ErbB4, and also to heterodimers of ErbB1/ErbB2, ErbB1/ErbB3, ErbB1/ErbB4, ErbB2/ErbB3, and ErbB2/ErbB4.[8] Our biochemical results indicated that BTC induced phosphorylation of all four of EGF receptors in VSMCs. Subsequently, BTC-evoked dual signaling cascades (1) prompt phosphorylation of Akt, GSK3, and FoxO factors, and nuclear accumulation of β-catenin and (2) transient phosphorylation of ERK/Elk1. Thus, on BTC binding, all possible dimeric EGR receptors may be activated, and their signals mediated accordingly. In comparison, AR is a specific ErbB1 ligand and binds preferentially to homodimeric ErbB1.[6] Accordingly, our biochemical results indicated that AR induced ErbB1 phosphorylation only. Subsequently, AR evoked relatively sustained ERK and Elk1 phosphorylation without any changes in Akt phosphorylation. Thus, BTC and AR evoke differential activation of EGF receptors and differential downstream signals in VSMCs (Figure 8).

The G1 phase of the cell cycle is controlled by D-type cyclins and cyclin-dependent kinases (CDKs).[20] Progression of G1 phase is mainly effected through induction of cyclin D1 by growth factors including EGF ligands.[20] Growth factor–induced activation of PI 3′-kinase/Akt and ERK has been linked to induction of cyclin D1 and cell cycle progression.[14] In the present study, we noted that BTC rapidly activated Akt in a PI 3′-kinase–dependent manner. Akt activation is known to lead to inactivation of GSK3α and β through their phosphorylation at Ser21 and Ser9, respectively.[21–23] GSK3 is a well-known regulator of cyclin D1 protein.[16,21–23] Active GSK3β-induced phosphorylation of cyclin D1 at Thr286 causes increased association of cyclin D1 with a nuclear exportin (Crm-1) and promotes nuclear exit and subsequent

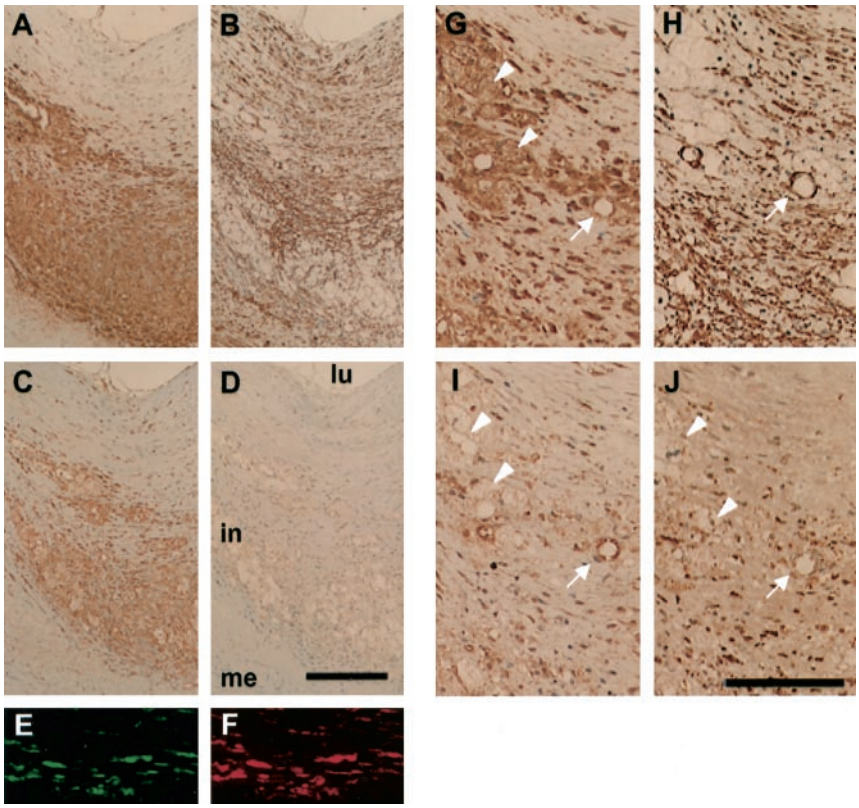

Figure 7. BTC and ErbB are found in atherosclerotic plaques. Atherosclerotic portion of a human coronary artery was immunostained for macrophages (A), VSMCs (B), BTC (C), and nonimmune rabbit immunoglobulins (D). BTC immunoreactivities were observed in the plaque where many macrophages and some VSMCs were accumulated. Double immunostaining of BTC (green fluorescence, E) and VSMCs (red fluorescence, F) showed that most VSMCs had BTC immunoreactivity near the inner elastic lamina in this lesion. Bar=200 μm; lu indicates lumen; in, intima; and me, media. Atherosclerotic portion of a human coronary artery was immunostained for macrophages (G), VSMCs (H), ErbB1 (I), and ErbB4 (J). In the plaque, many ErbB1- and ErbB4-positive cells were observed. However, macrophage-derived foam cells (arrowheads) showed no immunoreactivity to ErbB1 or ErbB4. VSMCs around a small vessel (arrow) were positive for ErbB1 immunostaining. Bar=100 μm.

proteasomal degradation of cyclinD1.[16] Conversely, inactivated GSK3β results in suppression of cyclin D1 phosphorylation at Thr286 and thereby suppresses cyclin D1 degradation. Akt is also known to phosphorylate all three FoxO subfamily of forkhead transcriptional factors, specifically FKHR, AFX, and FKHR1. This phosphorylation results in nuclear exclusion and inhibition of FoxO factor–mediated gene expression.[24] A recent report indicates that FoxO factors repress cyclin D1 expression at the transcriptional level.[19] Our results suggest that BTC-induced phosphorylation of FKHR and AFX may contribute to the increase in cyclin D1 at the transcription level by releasing the repression by FoxO factors. Thus, BTC-induced Akt activation contributes to the increase in cyclin D1 at the level of degradation and transcription by inducing the phosphorylation of GSK3β and FoxO factors (Figure 8).

Another important target of GSK3 is β-catenin,[22,25] a transcriptional coactivator that has important roles in early development. In unstimulated cells, active GSK3 constitutively phosphorylates β-catenin on N-terminal serine residues, targeting β-catenin for rapid ubiquitination and proteasome-mediated degradation.[26] Inhibition of GSK3-dependent phosphorylation of β-catenin allows β-catenin to accumulate in the cytoplasm and then translocate into the nucleus.[15] Once in the nucleus, β-catenin promotes transcription by binding to members of the lymphoid enhancer factor-1 (LEF-1)/T factor (TCF) family of DNA-binding proteins.[27,28] In mammalian cells, β-catenin upregulates the transcription of cyclin D1.[17,18] Thus, BTC-induced phosphorylated GSK3 can induce nuclear β-catenin accumulation, which increases induction of cyclin D1 mRNA transcription. In fact, our results showed that BTC rapidly phosphorylated GSK3 and induced nuclear β-catenin accumulation in a largely Akt-dependent manner in VSMCs. In addition, BTC induced cyclin D1 protein, DNA synthesis, and cell cycle progression in VSMCs. Accordingly, our results showed that pharmacological inhibition of PI 3′-kinase/Akt significantly suppressed BTC-induced cyclin D1 protein, DNA synthesis, and cell cycle progression, whereas MEK inhibition only slightly suppressed these BTC-induced processes. Taken together, our results indicate that PI 3′-kinase/Akt/GSK/FoxO/β-catenin cascades could be a major signaling mechanism by which BTC induces the upregulation of cyclin D1 protein and an increase in DNA synthesis and cell cycle progression (Figure 8).

Why was MEK inhibition unable to suppress BTC-induced cyclin D1, DNA synthesis, and cell cycle progression, even though BTC induced the MEK/ERK signaling cascade? Activation of the MEK/ERK pathway has been linked to the induction of cyclin D1. Sustained MEK/ERK activation is necessary for induction of cyclin D1 protein and DNA synthesis, whereas transient activation of the MEK/ERK signaling cascade may be insufficient to induce cyclin D1 protein and DNA synthesis.[14,29,30] In fact, our results showed that BTC-induced ERK phosphorylation was relatively transient. Thus, BTC-induced ERK activation could not be a major signaling pathway for induction of cyclin D1 protein and DNA synthesis in VSMCs. In comparison, our results indicate that AR-induced ERK1/2 activation is more sustained than BTC-induced ERK activation, whereas AR did not produce any change in Akt activation. Previous reports suggested that sustained ERK1/2 activation is a major deter-

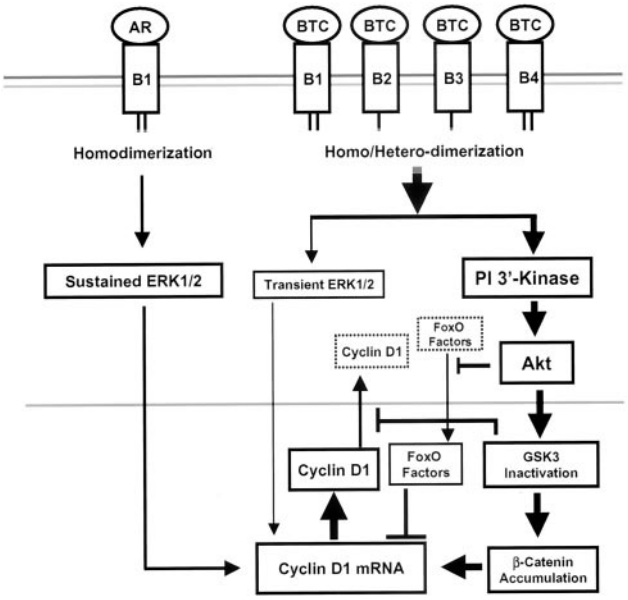

Figure 8. Mechanisms by which BTC and AR induce upregulation of cyclin D1 in VSMCs. In VSMCs, BTC binds to all four ErbB receptors, whereas AR binds only to the ErbB1 receptor. Formation of homo- and heterodimers among the ErbB receptors activates the PI 3′-kinase/Akt/GSK/β-catenin/FoxO factors cascade. This signaling cascade could be the main pathway for upregulation of cyclin D1 protein. BTC-induced transient activation of ERK1/2 is not sufficient for upregulation of cyclin D1 protein. Phosphorylated inactive GSKα/β not only suppresses cyclin D1 degradation through blocking of cyclin D1 mobilization from nucleus to cytosol, but also induces nuclear β-catenin accumulation, which increases cyclin D1 transcription. Mobilization of FoxO factors from cytoplasm to nucleus is inhibited by Akt-induced phosphorylation of FoxO factors. Therefore, FoxO factors induced repressive activity of cyclin D1 transcription in the nucleus is reduced. Meanwhile, AR-induced ErbB1 homodimerization evokes a sustained activation of ERK1/2, and this activation could be the main pathway for upregulation of cyclin D1 protein through induction of cyclin D1 transcription.

minant of upregulation of cyclin D1 protein and DNA synthesis in several cell types.[14,29,30] Likewise, our results suggest that sustained ERK/Elk1 activation could be a major signaling cascade for AR-induced upregulation of cyclin D1 protein and DNA synthesis in VSMCs. To support this idea, pharmacological inhibition of MEK significantly suppressed AR-induced cyclin D1 protein, DNA synthesis, and cell cycle progression, whereas PI 3′-kinase inhibition slightly suppressed AR-induced cyclin D1 protein, DNA synthesis, and cell cycle progression. Taken together, our results suggest that PI 3′-kinase/Akt/GSK3/FoxO/β-catenin cascades could be major signaling cascades for BTC-induced upregulation of cyclin D1 protein, DNA synthesis, and cell cycle progression, whereas a sustained ERK/Elk1 activation could be a major signaling cascade for AR-induced upregulation of cyclin D1 protein, DNA synthesis, and cell cycle progression (Figure 8).

Our immunolocalization study indicates that BTC, ErbB1, and ErbB4 are upregulated in the plaques of human atherosclerotic coronary artery. In these lesions, BTC is detected in macrophages and VSMCs, whereas ErbB1 receptor is detected in VSMCs. In the plaque shoulder, VSMCs are known to proliferate actively and to migrate from the media into the intima during the progression of atherosclerosis. BTC may contribute to the progression of atherosclerosis through autocrine and paracrine signaling. Several promising inhibitors for EGF receptors have recently been developed[31]; these inhibitors may prove useful for preventing the progression of atherosclerosis.

Acknowledgments

This work was supported by the Creative Research Initiatives of the Korean Ministry of Science and Technology and by the Brain Korea 21 Project. We thank Jennifer Macke for help in preparing the manuscript.

References

1. Shing Y, Christofori G, Ono Y, Sasada R, Igarashi K, Folkman J. Betacellulin: a mitogen from pancreatic beta cell tumors. *Science*. 1993; 259:1604–1607.
2. Sasada R, Ono Y, Taniyama Y, Shing Y, Folkman J, Igarashi K. Cloning and expression of cDNA encoding human betacellulin, a new member of the EGF family. *Biochem Biophys Res Commun*. 1993;190:1173–1179.
3. Shoyab M, McDonald VL, Bradley JG, Todaro GJ. Amphiregulin: a bifunctional growth-modulating glycoprotein produced by the phorbol 12-myristate 13-acetate-treated human breast adenocarcinoma cell line MCF-7. *Proc Natl Acad Sci U S A*. 1988;85:6528–6532.
4. Plowman GD, Green JM, McDonald VL, Neubauer MG, Disteche CM, Todaro GJ, Shoyab M. The amphiregulin gene encodes a novel epidermal growth factor-related protein with tumor-inhibitory activity. *J Cell Biol*. 1990;10:1969–1981.
5. Wells A. EGF receptor. *Int J Biochem Cell Biol*. 1999;31:637–643.
6. Olayioye MA, Neve RM, Lane HA, Hynes NE. The ErbB signaling network: receptor heterodimerization in development and cancer. *EMBO J*. 2000;19:3159–3167.
7. Gullick WJ. The Type 1 growth factor receptors and their ligands considered as a complex system. *Endocr Relat Cancer*. 2001;8:75–82.
8. Dunbar AJ, Goddard C. Structure-function and biological role of betacellulin. *Int J Biochem Cell Biol*. 2000;32:805–815.
9. Kim HS, Shin HS, Kwak HJ, Cho CH, Lee CO, Koh GY. Betacellulin induces angiogenesis through activation of mitogen-activated protein kinase and phosphatidylinositol 3′-kinase in endothelial cell. *FASEB J*. 2003;17:318–320.
10. Tamura R, Miyagawa J, Nishida M, Kihara S, Sasada R, Igarashi K, Nakata A, Yamamori K, Kameda-Takemura K, Yamashita S, Matsuzawa Y. Immunohistochemical localization of betacellulin, a member of epidermal growth factor family, in atherosclerotic plaques of human aorta. *Atherosclerosis*. 2001;155:413–423.
11. Shigematsu K, Koyama H, Olson NE, Cho A, Reidy MA. Phosphatidylinositol 3-kinase signaling is important for smooth muscle cell replication after arterial injury. *Arterioscler Thromb Vasc Biol*. 2000;20:2373–2378.
12. Braun-Dullaeus RC, Mann MJ, Seay U, Zhang L, von Der Leyen HE, Morris RE, Dzau VJ. Cell cycle protein expression in vascular smooth muscle cells in vitro and in vivo is regulated through phosphatidylinositol 3-kinase and mammalian target of rapamycin. *Arterioscler Thromb Vasc Biol*. 2001;21:1152–1158.
13. Ahn JD, Morishita R, Kaneda Y, Lee SJ, Kwon KY, Choi SY, Lee KU, Park JY, Moon IJ, Park JG, Yoshizumi M, Ouchi Y, Lee IK. Inhibitory effects of novel AP-1 decoy oligodeoxynucleotides on vascular smooth muscle cell proliferation in vitro and neointimal formation in vivo. *Circ Res*. 2002;90:1325–1332.
14. Roovers K, Assoian RK. Integrating the MAP kinase signal into the G1 phase cell cycle machinery. *Bioessays*. 2000;22:818–826.
15. Funayama N, Fagotto F, McCrea P, Gumbiner BM. Embryonic axis induction by the armadillo repeat domain of β-catenin: evidence for intracellular signaling. *J Cell Biol*. 1995;128:959–968.
16. Alt JR, Cleveland JL, Hannink M, Diehl JA. Phosphorylation-dependent regulation of cyclin D1 nuclear export and cyclin D1-dependent cellular transformation. *Genes Dev*. 2000;14:3102–3114.
17. Shtutman M, Zhurinsky J, Simcha I, Albanese C, D'Amico M, Pestell R, Ben-Ze'ev A. The cyclin D1 gene is a target of the β-catenin/LEF-1 pathway. *Proc Natl Acad Sci U S A*. 1999;96:5522–5527.
18. Tetsu O, McCormick F. β-Catenin regulates expression of cyclin D1 in colon carcinoma cells. *Nature*. 1999;398:422–426.

19. Schmidt M, Fernandez de Mattos S, van der Horst A, Klompmaker R, Kops GJ, Lam EW, Burgering BM, Medema RH. Cell cycle inhibition by FoxO forkhead transcription factors involves downregulation of cyclin D. *Mol Cell Biol*. 2002;22:7842–7852.
20. Sherr CJ. G1 phase progression: cycling on cue. *Cell*. 1994;79:551–555.
21. Cross DA, Alessi DR, Cohen P, Andjelkovich M, Hemmings BA. Inhibition of glycogen synthase kinase-3 by insulin mediated by protein kinase B. *Nature*. 1995;378:785–789.
22. Cohen P, Frame S. The renaissance of GSK3. *Nat Rev Mol Cell Biol*. 2001;2:769–776.
23. Hardt SE, Sadoshima J. Glycogen synthase kinase-3β: a novel regulator of cardiac hypertrophy and development. *Circ Res*. 2002;90:1055–1063.
24. Brunet A, Bonni A, Zigmond MJ, Lin MZ, Juo P, Hu LS, Anderson MJ, Arden KC, Blenis J, Greenberg ME. Akt promotes cell survival by phosphorylating and inhibiting a Forkhead transcription factor. *Cell*. 1999;96:857–868.
25. Peifer M, Polakis P. Wnt signaling in oncogenesis and embryogenesis: a look outside the nucleus. *Science*. 2000;287:1606–1609.
26. Orford K, Crockett C, Jensen JP, Weissman AM, Byers SW. Serine phosphorylation-regulated ubiquitination and degradation of β-catenin. *J Biol Chem*. 1997;272:24735–24738.
27. Hsu SC, Galceran J, Grosschedl R. Modulation of transcriptional regulation by LEF-1 in response to Wnt-1 signaling and association with β-catenin. *Mol Cell Biol*. 1998;18:4807–4818.
28. Behrens J, von Kries JP, Kuhl M, Bruhn L, Wedlich D, Grosschedl R, Birchmeier W. Functional interaction of β-catenin with the transcription factor LEF-1. *Nature*. 1996;382:638–642.
29. Roovers K, Davey G, Zhu X, Bottazzi ME, Assoian RK. $\alpha_5\beta_1$ integrin controls cyclin D1 expression by sustaining mitogen-activated protein kinase activity in growth factor-treated cells. *Mol Biol Cell*. 1999;10:3197–3204.
30. Bottazzi ME, Zhu X, Bohmer RM, Assoian RK. Regulation of p21(cip1) expression by growth factors and the extracellular matrix reveals a role for transient ERK activity in G1 phase. *J Cell Biol*. 1999;146:1255–1264.
31. Ciardiello F, Tortora G. A novel approach in the treatment of cancer: targeting the epidermal growth factor receptor. *Clin Cancer Res*. 2001;7:2958–2970.

Betacellulin and Amphiregulin Induce Upregulation of Cyclin D1 and DNA Synthesis Activity Through Differential Signaling Pathways in Vascular Smooth Muscle Cells

Hyoung Seek Shin, Hyo Jeong Lee, Makoto Nishida, Mi-Sook Lee, Ritsu Tamura, Shizuya Yamashita, Yuji Matsuzawa, In-Kyu Lee and Gou Young Koh

Circ Res. 2003;93:302-310; originally published online July 17, 2003;
doi: 10.1161/01.RES.0000086803.64109.9E
Circulation Research is published by the American Heart Association, 7272 Greenville Avenue, Dallas, TX 75231

Print ISSN: 0009-7330. Online ISSN: 1524-4571

Online Supplementary

Betacellulin and Amphiregulin Induce Up-regulation of Cyclin D1 and DNA Synthetic Activity Through Differential Signaling Pathways in Vascular Smooth Muscle Cells

(Mitogenic role of BTC and AR)

Hyoung Seek Shin, Hyo Jeong Lee, Makoto Nishida, Mi Sook Lee, Ritsu Tamura, Shizuya Yamashita, Yuji Matsuzawa, In-Kyu Lee, Gou Young Koh

National Creative Research Initiatives Center for Endothelial Cells and Division of Molecular and Life Sciences, Pohang University of Science and Technology, Pohang, 790-784, Korea (H.S.S., M.S.L., G.Y.K.)
Department of Internal Medicine, Keimyung University School of Medicine, Taegu, 700-712, Korea (H.J.L, I-K.L.)
Department of Internal Medicine and Molecular Science, Graduate School of Medicine, Osaka University, 2-2, Yamada-Oka, Suita, Osaka, 565-0871, Japan (M.N., R.T., Y.M., S.Y.)

Subject Codes: 96, 134, 138, 147, 162

Correspondence to:
Gou Young Koh, M.D., Ph.D.
National Creative Research Initiatives Center for Endothelial Cells
Division of Molecular and Life Sciences
Pohang University of Science and Technology
San 31, Hyoja-Dong, Pohang, 790-784,
Republic of Korea
Phone: 82-54-279-2286; Fax: 82-54-279-8366
e-mail: gykoh@postech.ac.kr

Supplementary Materials and Methods

Materials and Cell Culture

Recombinant human BTC and AR were purchased from Sigma-Aldrich Inc (St. Louis, MO). Recombinant human EGF was purchased from R&D Systems (Minneapolis, MN). PI 3'-kinase inhibitor wortmannin, Akt inhibitor (1L-6-hydroxymethyl-chiro-inositol 2(R)-2-O-methyl-3-O-octadecylcarbonate, a phosphatidylinositol ether analog that potently and selectively inhibits Akt, IC_{50} = 5.0 μM) (1) and mitogen-activated protein/extracellular signal-regulated kinase (MEK) 1/2 inhibitor PD98059 were obtained from Calbiochem, Inc (San Diego, CA). Antibodies for phospho-specific Akt (Ser473), GSK3α/β (Ser21/Ser9), FKHR (Ser256)/AFX, Elk1 (Ser383) and ERK1/2 (Thr202/Tyr204) were purchased from Cell Signaling Technology (Beverly, MA). Antibodies for ErbB1, ErbB2, ErbB3, ErbB4, and cyclin D1 were purchased from Santa Cruz Biotechnology (Santa Cruz, CA). Antibodies for phospho-ErbB1, phospho-ErbB2, and phospho-tyrosine were purchased from Upstate Biotechnology (Lake Placid, NY). Antibody for β-catenin was purchased from BD Transduction Laboratories (San Diego, CA). Cell culture products and most other biochemical reagents were purchased from Sigma-Aldrich Inc., unless otherwise specified. HTASMCs were isolated from thoracic aortas of donors during heart transplant by the explant method (2,3). Tissue collection was approved by the local Ethics Committee. Purity of HTAVSMCs was characterized by positive staining with smooth muscle–specific α-actin monoclonal antibodies (Sigma-Aldrich Inc). These HTAVSMCs were maintained in Dulbecco's modified Eagle's medium (DMEM) supplemented with 10% (vol/vol) fetal bovine serum (FBS) at 37°C in 5% CO_2. The primary cultured cells used in this study were between passage

3 and 5.

Biochemical Analyses

HTAVSMCs were incubated in DMEM with 1% fetal bovine serum (FBS) for 16 hr before addition of the indicated growth factors. To measure phosphorylations of ErbB1, ErbB2, Akt (Ser473), GSK3α/β, ERK1/2 and Elk1, and protein levels of β-catenin and cyclin D1, HTAVSMCs were treated with BTC or AR for the indicated times and doses. The treated HTAVSMCs were washed 2 times with PBS, dissolved in sample buffer (50 mM Tris-HCl, 100 mM NaCl, 0.1% SDS, 1% NP-40, 50 mM NaF, 1 mM Na_3VO_4, 1 μg/ml aprotinin, and 1 μg/ml pepstatin, and 1 μg/ml leupeptin), boiled, separated by SDS-PAGE, and transferred to nitrocellulose membrane. The phosphorylation and protein levels analyzed according to the manufacturer's protocol {Upstate Biotechnology for ErbB1 and ErbB2; New England BioLabs for Akt (Ser473), GSK3α/β, ERK1/2 and Elk1}. Nuclear fractions for measuring nuclear β-catennin level were obtained as previously described (4). To measure the phosphorylation of ErbB3 or ErbB4, 1.0 mg of cell lysate protein was immunoprecipitated with anti-ErbB3 or ErbB4 (Santa Cruz Biotechnology, Inc.). Immunoprecipitates were western blotted with anti-phosphotyrosine antibody (Upstate Biotechnology), and the membrane was reprobed with anti-ErbB3 antibody or anti-ErbB4 antibody to verify equal loading of protein in each lane. All signals were visualized and analyzed by densitometric scanning (LAS-1000, Fuji Film, Tokyo).

Confocal Microscopy

HTAVSMCs were seeded onto glass coverslips and incubated for 24 hr before

addition of BTC. Treated cells were washed with PBS, fixed with methanol/acetone (1:1) for 15 min, incubated with anti-β-catenin antibody (BD Transduction Laboratories, San Diego, CA), then incubated with FITC-conjugated secondary antibody, and counter-stained with Hoechst 33425. The slides were mounted and examined by confocal microscope, and images were captured with LSM 510 (Zeiss, Gottingen, Germany).

RPA

The partial cDNA of human cyclin D1 (nucleotides 383-865, GenBank accession BC023620) was amplified by PCR and subcloned into pBluescript II KS+ (Stratagene). After linearizing with EcoRI, ^{32}P-labeled antisense RNA probes were synthesized by *in vitro* transcription using T7 polymerase (Ambion Maxiscript kit) and gel purified. RPA was performed on total RNAs using the Ambion RPA kit. An antisense RNA probe of human cyclophilin (nucleotides 135-239, GenBank accession X52856) was used as an internal control for RNA quantification.

Assays of DNA synthesis and cell cycle progression

The DNA synthetic activity of HTAVSMCs was measured as previously described (4). Briefly, HTAVSMCs were plated onto 24-well plates at a density of 2 x 10^4 cells/cm^2 in DMEM medium supplemented with 10% (vol/vol) FBS. After 12 hr in culture, the control buffer, BTC (10 ng/ml) or AR (100 ng/ml) in the absence and presence of PD98059 (PD, 50 nM) or wortmannin (WT, 30 nM) was added in DMEM supplemented with 2% serum. At 24 and 48 hr, the same reagents were refreshed. At 72 hr, the cells were washed twice with PBS, and the DNA amount was measured with

PicoGreen fluorescent reagent (Molecular Probes, Eugene, OR) according to the method described by Singer *et al.* (6) using a fluorescence spectrometer equipped with a microplate reader (Molecular Device, Sunnyvale, CA). Treated cells were trypsinized and then fixed with ice-cold 70% ethanol. The fixed cells were washed with PBS and resuspended in PBS containing 1 mg/ml propidium iodide plus 0.1% RNase. DNA fluorescence was measured with a FACSCalibur (Becton Dickinson).

Sampling and immunohistochemistry

Human coronary arteries were obtained from autopsied cases with informed consent of the next of kin. The tissues were fixed with 10% phosphate-buffered formalin for 4–6 hr at 4°C and embedded in paraffin. Immunohistochemical detection of BTC, smooth muscle actin and EGF receptors was performed as described previously (7). Briefly, the paraffin sections (about 4 μm thick) were de-paraffinized, treated with 3% H_2O_2 for 5 min, blocked with BSA for 20 min, and incubated with rabbit polyclonal anti-BTC antibody (a gift from Dr. Reiko Sasada in Takeda Chemical Industries, Tsukuba, Japan), mouse monoclonal anti-α-isoform of VSMC antibody and mouse anti-ErbB2 antibody (Histofine, Nichirei Co., Ltd, Tokyo, Japan), mouse anti-macrophage antibody (DAKO, Glostrup, Denmark), mouse monoclonal anti-ErbB1 antibody (Cambridge Research Biochemicals, London, UK), or mouse anti-ErbB4 antibody (Chemicon, Temecula, CA). Then the slides were incubated with secondary antibody and visualized with 3-amino-9-ethylcarbazol or 3, 3'-diaminobenzidine according to manufacturer's instruction (DAKO), and counterstained with Mayer's hematoxylin. Double immunofluorescence stainings of BTC and VSMCs was performed using Alexa 488 anti-rabbit IgG and Alexa 594 anti-mouse IgG (Molecular Probe, Eugene, OR) as secondary antibodies.

Data analyses

Data are expressed as mean ± standard deviation (SD). Statistical significance was tested using 1-way ANOVA followed by the Student-Newman-Keuls test. Statistical significance was set at $p<0.05$.

References

1. Hu Y, Qiao L, Wang S, Rong SB, Meuillet EJ, Berggren M, Gallegos A, Powis G, Kozikowski AP. 3-(Hydroxymethyl)-bearing phosphatidylinositol ether lipid analogues and carbonate surrogates block PI3-K, Akt, and cancer cell growth. *J Med Chem.* 2000;43:3045-3051.
2. Dubey RK, Gillespie DG, Mi Z, Jackson EK. Adenosine inhibits growth of human aortic smooth muscle cells via A2b receptors. *Hypertension.* 1998;31:516–521.
3. Ahn JD, Morishita R, Kaneda Y, Lee SJ, Kwon KY, Choi SY, Lee KU, Park JY, Moon IJ, Park JG, Yoshizumi M, Ouchi Y, Lee IK. Inhibitory effects of novel AP-1 decoy oligodeoxynucleotides on vascular smooth muscle cell proliferation in vitro and neointimal formation in vivo. *Circ Res.* 2002;90:1325-1332.
4. Dignam JD, Lebovitz RM, Roeder RG. Accurate transcription initiation by RNA polymerase II in a soluble extract from isolated mammalian nuclei. *Nucleic acids Res.*1983;11:1475-1489.
5. Chae JK, Kim I, Lim ST, Chung MJ, Kim WH, Kim HG., Ko JK, Koh GY. Co-administration of angiopoietin-1 and vascular endothelial growth factor enhances collateral vascularization. *Arterioscler Thromb Vasc Biol.* 2000;20:253-2578.
6. Singer VL, Jones LJ, Yue ST, Haugland RP. Characterization of PicoGreen reagent and development of a fluorescence-based solution assay for double-stranded DNA quantitation. *Anal Biochem.* 1997;249:228-238.
7. Tamura R, Miyagawa J, Nishida M, Kihara S, Sasada R, Igarashi K, Nakata A, Yamamori K, Kameda-Takemura K, Yamashita S, Matsuzawa Y.

Immunohistochemical localization of Betacellulin, a member of epidermal growth factor family, in atherosclerotic plaques of human aorta. *Atherosclerosis.* 2001;155:413-423.

Online Supplementary Figure legends

Figure 1. BTC induces the phosphorylation of ErbB1, ErbB2, ErbB3, and EbB4. HTASMCs were incubated for 16 hours in medium with 1% serum-containing DMEM. **A**, The cells were treated with control buffer (CB) or BTC (1 and 10 ng/ml) for 3 min, and cell lysates were harvested. Each lane contains 50 μg of total protein. Blots were probed with anti-phospho-ErbB1/B2 (upper panel). The membrane was stripped and reprobed with anti-ErbB1/2 antibody (lower panel) to verify equal loading of protein in each lane. **B** and **C**, The cells were treated with control buffer (CB) or BTC (10 ng/ml) for 3 min and cell lysates were harvested in extraction buffer, and 0.5 mg of protein was used for immunoprecipitation with anti-ErbB3 or anti-ErbB4 antibody. Immunoprecipitated samples were blotted with anti-phosphotyrosine antibody (upper panels). The membranes were reprobed with anti-ErbB3 or anti-ErbB4 antibody to verify equal loading of protein in each lane (lower panels). Results were similar in three independent experiments. **Fold:** Densitometric analyses are presented as the relative ratio of phospho-ErbB1/2/3/4 to ErbB1/2/3/4. The relative ratio measured to control buffer (CB) is arbitrarily presented as 1. Numbers represent the mean ± S.D. from 3 experiments. *, $p<0.05$ *versus* CB.

Figure 2. BTC and AR increase DNA synthesis and cell cycle progression. HTASMCs were plated in DMEM supplemented with 10% serum. After 12 hr in culture, the control buffer (CB), BTC (10 ng/ml) or AR (100 ng/ml) in the absence and presence of PD98059 (PD, 50 nM) or wortmannin (WT, 30 nM) was added in DMEM supplemented with 2% serum. At 24 and 48 hr, the same reagents were refreshed. **A**, At 72 hr, the DNA amount was measured with PicoGreen fluorescent reagent. Bars represent the mean ± S.D. from 6 experiments. *, $p<0.05$ *versus* CB; $^{\#}$, $p<0.05$ *versus* BTC (10 ng/ml) or AR (100 ng/ml). **B**, At 48 hr, the cells were harvested and stained with propidium iodide, and cell cycle progression was determined by FACS analysis. The X-axis shows DNA content, and the Y-axis shows the number of cells.

Online Figure 1. Shin et al.

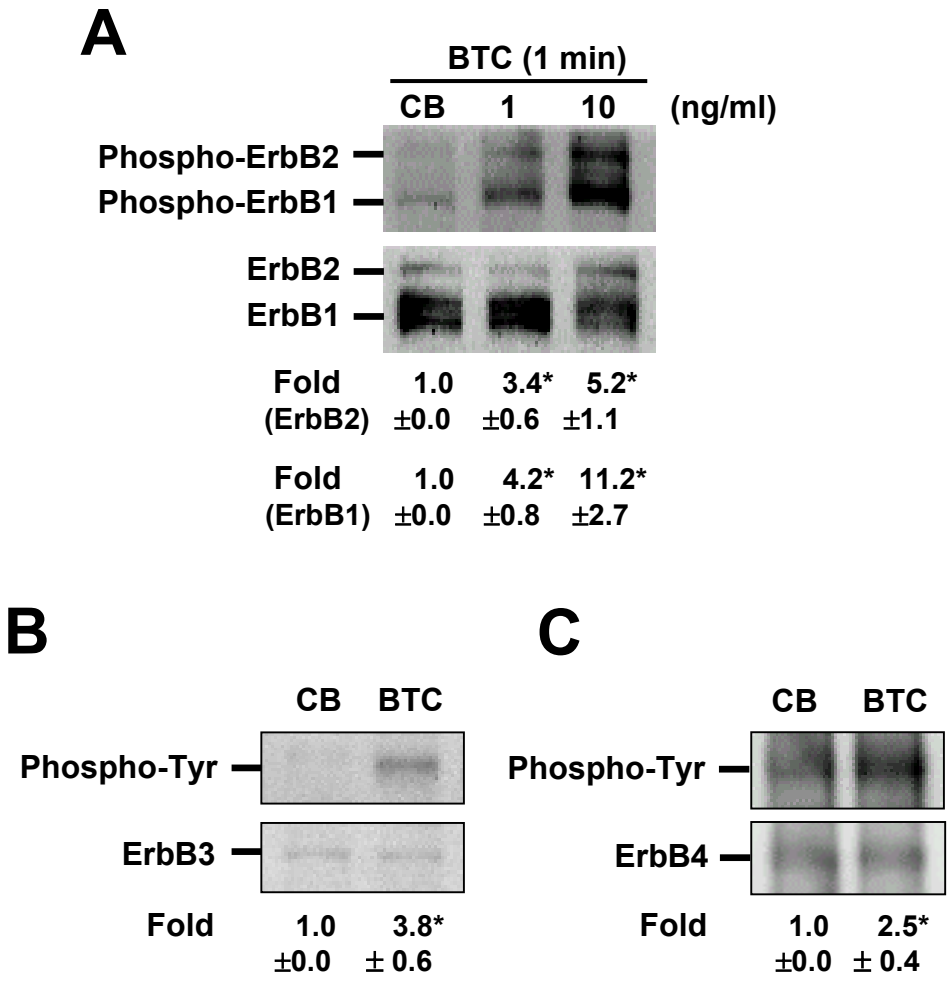

Online Figure 2. Shin et al.